Journal of Colloid and Interface Science 446 (2015) 24–30

Contents lists available at ScienceDirect

Journal of Colloid and Interface Science

www.elsevier.com/locate/jcis

Fullerene oxidation and clustering in solution induced by light

Rajeev Dattani [a,b], Kirsty F. Gibson [b], Sheridan Few [a,c], Aaron J. Borg [b], Peter A. DiMaggio [b], Jenny Nelson [a,c], Sergei G. Kazarian [b], João T. Cabral [a,b,*]

[a] Centre for Plastic Electronics, Imperial College London, London SW7 2AZ, United Kingdom
[b] Department of Chemical Engineering, Imperial College London, London SW7 2AZ, United Kingdom
[c] Department of Physics, Imperial College London, London SW7 2AZ, United Kingdom

GRAPHICAL ABSTRACT

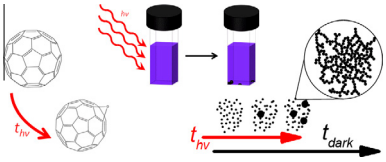

ARTICLE INFO

Article history:
Received 24 November 2014
Accepted 5 January 2015
Available online 22 January 2015

Keywords:
Fullerene
Aggregation
Light exposure
Oxidation
C_{60}
Epoxide

ABSTRACT

We investigate the environmental stability of fullerene solutions by static and dynamic light scattering, FTIR, NMR and mass spectroscopies, and quantum chemical calculations. We find that visible light exposure of fullerene solutions in toluene, a good solvent, under ambient laboratory conditions results in C_{60} oxidation to form fullerene epoxides, and subsequently causes fullerene clustering in solution. The clusters grow with time, even in absence of further illumination, and can reach dimensions from ≈100 nm to the μm scale over ≈1 day. Static light scattering suggests that resulting aggregates are fractal, with a characteristic power law (d_f) that increases from approximately 1.3 to 2.0 during light exposure. The clusters are bound by weak Coulombic interactions and are found to be reversible, disintegrating by mechanical agitation and thermal stress, and reforming over time. Our findings are relevant to the solution processing of composites and organic photovoltaics, whose reproducibility and performance requires control of fullerene solution stability under storage conditions.

1. Introduction

Since the advent of large scale fullerene production [1], photo-polymerisation and -oxidation has been reported for C_{60} fullerenes and their derivatives in the solid state [2] and is now relatively well understood [2–5]. By contrast, the environmental stability of fullerene solutions, despite its relevance for plastic electronics [6] and fullerene-based composites [7], has received comparatively less attention. Three outcomes have been reported for the light exposure of C_{60} solutions: degradation of the fullerene cage [8,9], photo-polymersation [10] and oxidation [10] whilst others have reported aggregation with considering light exposure [11–15].

Degradation of the fullerene cage (photolysis) has been found by UV radiation in hexane [8,9], eventually leading to the formation of a brown deposit which could not be re-dissolved [8]. Fullerene photo-polymerisation and -oxidation upon UV exposure has been investigated in a variety of chlorinated and saturated hydrocarbon solvents, in ambient and inert atmospheres [10]. UV light was found to cause photo-oxidation in saturated hydrocarbon solvents and ambient conditions, while fullerene photo-polymerisation was reported to occur in chlorinated solvents in inert

* Corresponding author at: Department of Chemical Engineering, Imperial College London, London SW7 2AZ, United Kingdom.
E-mail addresses: rajeev.dattani10@imperial.ac.uk (R. Dattani), k.gibson@imperial.ac.uk (K.F. Gibson), sheridan.few10@imperial.ac.uk (S. Few), a.borg12@imperial.ac.uk (A.J. Borg), p.dimaggio@imperial.ac.uk (P.A. DiMaggio), j.nelson@imperial.ac.uk (J. Nelson), s.kazarian@imperial.ac.uk (S.G. Kazarian), j.cabral@imperial.ac.uk (J.T. Cabral).

http://dx.doi.org/10.1016/j.jcis.2015.01.005
0021-9797/

atmosphere. The formation of a brown deposit was then rationalised as arising from fullerene 'polymer'. Similar UV spectroscopy data at wavelengths of 330 and 400 nm has, however, been interpreted as either evidence of decomposition [9,8] or polymerisation [10]. Discriminating between these results appears thus difficult via UV spectroscopy, and both fullerene degradation and photopolymerisation remain rather poorly understood.

Although fullerene aggregation in solution has been previously reported [11,12,15,13,14], its trigger and mechanism have not yet been elucidated. Ying et al. [11,12] studied fullerene/benzene solutions over a 40–90 day period using static and dynamic light scattering. An increase in scattering intensity over time was found, which was reversed upon hand shaking the solution. A laser wavelength of 790 nm (and power of 30 mW) was assumed to be sufficiently away from the UV region in which degradation or polymerisation had been reported to occur, although fullerene oxidation is likely to take place close to this wavelength range [16]. Solution storage between measurements, in terms of light exposure and solution atmosphere, was not discussed but the formation of an insoluble brown residue was also observed. All solution concentrations in the above studies were below the reported solubility limits [17] and agglomeration was thus not expected. Mixed solvent systems containing toluene and acetonitrile [14] or aqueous electrolyte solutions [15] have been found to cause C_{60} cluster formation and crystallisation with various crystal symmetries [18], but are beyond the scope of the present study.

Several mechanisms can potentially describe fullerene aggregation, according to rate limiting factors and fractal geometry. Generally, these include reaction-limited and diffusion-limited aggregation and, within these, models for monomer–cluster and cluster–cluster aggregation [19]. Reaction-limited aggregation has typical energy barriers of $\approx 10\ k_BT$ [20] which must be overcome for aggregation to occur, whereas diffusion-limited aggregation is effectively barrier-less and the aggregation process is limited by the cluster diffusion. A characteristic fractal power law (d_f) found from an elastic scattering experiment $I \propto q^{-d_f}$, where q is wavenumber, distinguishes the two regimes as both yield characteristic structures. Reaction-limited monomer–cluster aggregation, otherwise known as the Eden model [21] and diffusion-limited monomer–cluster aggregation [22] both result in more compact structures, characterised by a higher d_f of 3 and 2.5 respectively, compared to their cluster–cluster analogues [19]. A 'poisoned' Eden model [23,24] describes the aggregation of primary particles that are not only limited by a reaction step, but also by a limited number of possible sites where aggregation can take place. A crossover from reaction-limited to diffusion-limited mechanisms can also be expected [25,20], as the growing clusters become increasingly hindered diffusion through the solvent, as opposed to the sticking probability between individual particles. This mechanism predicts a decreasing d_f as agglomeration proceeds, typically from 2.1 to 1.8 [25].

In this work, we probe the light-induced oxidation and subsequent clustering of C_{60} in toluene via static and dynamic light scattering alongside analytical techniques and computational calculations of the factors governing fullerene association.

2. Materials and methods

Neat C_{60} fullerenes (99% MER Corp) were dissolved in toluene (99.5%, VWR), at various concentrations below the reported miscibility limit (0.32 wt%) [17]. All solution vials were wrapped in aluminium foil to minimise ambient light exposure prior to controlled light exposure. Four light sources were evaluated, specifically: a 633 nm, 4 mW, HeNe laser, a 100 W, Mercury UV-A (365 nm) lamp, a high intensity white light, and ambient laboratory light (detailed in Section S3). The most effective light source was found to be the red laser source, with the highest irradiance, and was thus employed for most experiments reported in this study. Exposure times ranged from 0 to 25 h in a 1 cm rectangular quartz cuvette (Hellma) sealed with PTFE tape and a screw-top lid to prevent evaporation. All experiments were carried out with 1 ml of solution at 25 °C, unless otherwise specified. Prior to measurements the C_{60}/toluene solutions were filtered through a 220 nm PTFE filter (VWR) to remove dust and particulates. Dynamic Light Scattering (DLS) was performed in the same cuvette using a Malvern Nano-S with a fixed angle detector at $\theta = 173°$, corresponding to $q = 2.96 \times 10^{-2}\ \text{nm}^{-1}$, where $q = \frac{4\pi n}{\lambda} \sin\frac{\theta}{2}$, and n, λ and θ are the refractive index of the solvent (1.496), laser wavelength (633 nm) and scattering angle (173°) respectively. The field correlation function $g^{(1)}(t)$ obtained from DLS was fit with a series of exponentials using[1]:

$$g^{(1)}(t) = \sum_{i=1}^{N} a_i(q) \exp(-\Gamma_i t) \tag{1}$$

where a_i is the scattering amplitude of the ith mode, and Γ_i is the mean inverse relaxation time of each diffusive mode, with $N \leq 3$. The diffusion coefficient D_i of each mode is computed from $\Gamma_i = D_i q^2$ and the hydrodynamic radius, $R_{h,i}$, of the particles is obtained from the Stokes–Einstein equation:

$$R_{h,i} = \frac{k_B T}{6\pi\eta D_i} \tag{2}$$

where k_B is the Boltzmann constant, T is the temperature and η is the dynamic viscosity of the solvent, for toluene (5.5×10^{-4} Pa s for toluene at 25 °C). In order to reproducibly fit the various decay modes, the fastest decay (Γ_1) was fixed, as it is present in neat toluene as well as fullerene solutions and cannot be interpreted quantitatively. A contribution from molecular C_{60}, expected at the nanosecond time scale is not resolved reliably, likely due to its low content in solution (bound by its low miscibility in toluene) and limited detector sensitivity. The second decay (Γ_2) was assigned to clusters which form upon illumination with dimensions $R_{h,2}$ of the order of 100 nm. The final decay (Γ_3) yields $R_{h,3}$ on the order of 10 μm, beyond the limit of Brownian diffusion analysis. It is common for long decay times detected by DLS, corresponding to particulates of dimensions on the order of 10 μm, to be ascribed to contaminants; however, due to the trend observed during light exposure, and their initial absence in the filtered solution, we interpret them as large C_{60} clusters. These larger particles can eventually be observed in solution via transmission optical microscopy (Olympus BX71), confirming the formation of large clusters of 10–90 μm dimensions. The amplitude of each mode, a_1, a_2 and a_3 is also computed, quantifying their relative population. The three modes, characteristic $R_{h,i}$, and attributed physical meaning are summarised in Table 1. Mass spectroscopy (LTQ Velos Pro, Thermo Scientific), FTIR (Bruker Tensor 27) and NMR (Av500) spectroscopies were used to characterise light exposed C_{60} solutions. Quantum chemical calculations were carried out on pairs of $C_{60}O_x$ molecules. Further details of these analytical techniques, computational methods and sample preparation can be found in Section S1.

[1] Γ_i is the mean inverse relaxation time of diffusive modes with the z-averaged translational diffusion coefficient $D_i = \Gamma_i/q^2$. For the case of two or three well-separated modes, DLS data can be adequately modeled with double- or triple-exponentials ($N = 2$ or 3). This allocates one exponential per mode and hence allows for a statistically robust estimate of the z-averaged particle size and of the corresponding partial scattering intensity of the respective mode.

Table 1
Summary of fitting parameters, size regimes and species.

Mode	Amplitude	R_h Regime/nm	Attributed to
1st	a_1	0.05±0.01	Solvent
2nd	a_2	50–200	Clusters
3rd	a_3	10,000–90,000	Large clusters

3. Results and discussion

As discussed above, three outcomes of light exposure to C_{60}, degradation, polymerisation and oxidation, may be expected. The first two are changes in the chemical species which generally occur upon UV irradiation. Visible light has been shown to induce C_{60} photo-chemical transformations and have been shown to have a low energy gap of approximately 1.8 eV, which excites ground state electrons in C_{60} to the excited state and causes oxidation in the presence of oxygen [16,26]. Our expectation is therefore to observe phenomena associated with fullerene oxidation, and is indeed confirmed by spectroscopic data.

3.1. Fullerene epoxidation

MS (Fig. 1a) indicates the presence of $C_{60}O$, $C_{60}O_2$ and $C_{60}O_3$, and the NMR spectrum shows a peak at δ 49 ppm, corresponding to epoxide formation, and absence of peaks in the 180–220 ppm region characteristic of carbonyl groups. A ratio of peak intensities indicates approximately 0.7% epoxide formation, after 21 h of light exposure (Fig. S1). By MS, no additional peaks corresponding to a mass lower than one individual fullerene molecule were present in a solution exposed to light indicating that photolysis is not taking place. Due to the relatively slow formation of $C_{60}O_x$, a significantly longer exposure time of 2 weeks was employed for FTIR spectroscopy samples in order to increase the concentration of oxidised fullerene. Upon light exposure, peaks were observed at 806, 1018, 1095, 1261 and 1459 cm^{-1} which have been previously assigned to fullerene epoxide formation [27–29], either for $C_{60}O$ or $C_{60}O_3$ as indicated on Fig. 1b ($C_{60}O_2$ was not observed by FTIR spectroscopy, but was shown to be present by MS). The potential outcomes of degradation and polymerisation can now be ruled out, as no brown residue nor supporting spectroscopic evidence was found [8,10]. We thus conclude via MS, FTIR spectroscopy and NMR that the exposure of fullerene to light (633 nm, 4 mW) results in fullerene epoxide formation. The mechanism for C_{60} oxidation has been described previously [16,26], and is briefly summarised here. The incoming photon (1.8 eV) excites an electron in the C_{60} to the first excited state, followed by internal conversion and inter-system crossing to form a triplet excited state; in the presence of oxygen, triplet energy transfer occurs and produces singlet oxygen; the simultaneous presence of triplet excited state C_{60} and singlet oxygen then produces fullerene oxide.

3.2. Epoxide aggregation

The ensuing aggregation of oxidised fullerenes in toluene upon light exposure was investigated via DLS. A comparison of a freshly prepared and a control solution of two week old 0.3 wt% C_{60}/toluene solution stored in the dark is shown in Fig. 1c. Solutions aged in the dark (•) and freshly prepared (■) exhibit similar scattering profiles. These are distinct from the multi-step decay functions, seen in Fig. 1d for light exposed C_{60} solutions. Typical correlation functions, $g^{(1)}(q,t)$, fitted to Eq. (1) show the emergence of a second and third decay during light exposure, both of which continue to show an increase in intensity and $R_{h,2}$ with light

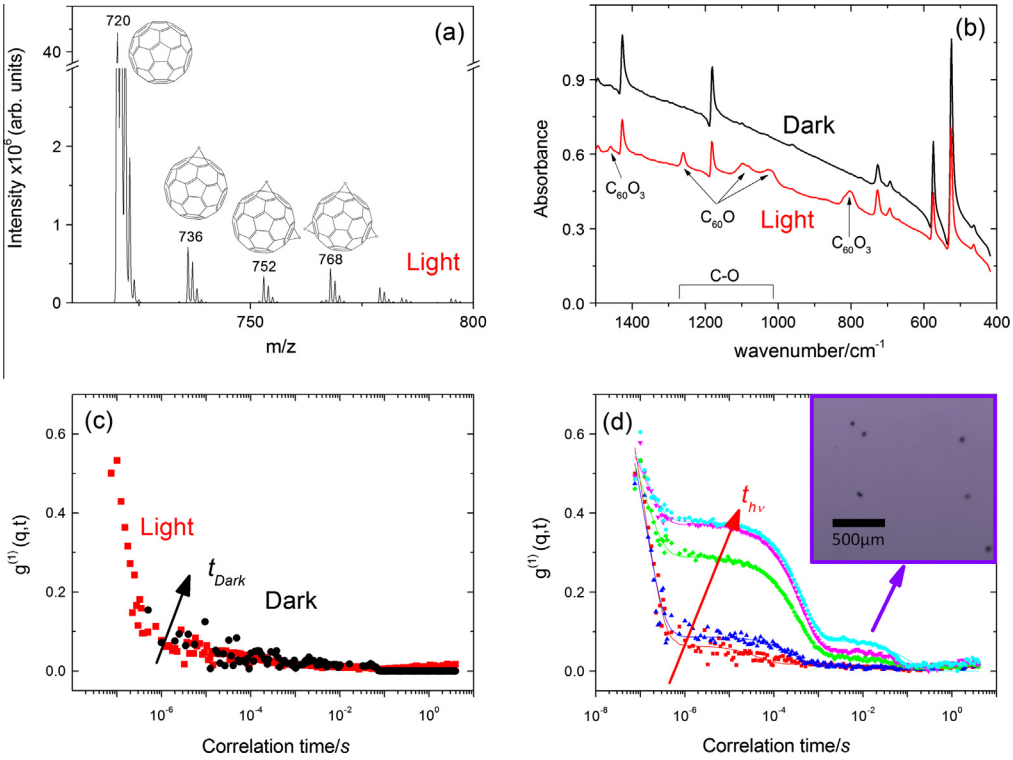

Fig. 1. (a) Mass spectroscopy results of C_{60}/toluene solution exposed for 21 h (and diluted with IPA for injection), where peaks corresponding to $C_{60}O_x$ with $x = 0$–3 are illustrated with possible epoxides formed. (b) FTIR spectra of C_{60} solution prior and after 2-week light exposure ($C_{60}O_x$) and embedded in KBr discs. (c) DLS correlation function of a freshly prepared (■) 0.3 wt% C_{60}/toluene solution, and following ageing in the dark for 14 days (•). (d) DLS correlation function of 0.3 wt% C_{60}/toluene solutions at light exposure times: $t = 0$ (■), 1 (▲), 5 (◆), 15 (▼), 20 (●) h. Solid lines are fits to Eq. (1). A second and third decays appears after, respectively, 1 h and 5 h. Inset shows transmission optical microscope image of micron-scale $C_{60}O_x$ clusters observed after 16 h light exposure.

exposure time (t_{hv}). The emergence of well defined clusters is thus evidently the result of fullerene photo-oxidation.

In order to quantify and understand the interactions between fullerene epoxide (and fullerene) molecules, quantum chemical calculations were carried out, as detailed in Section S1.3. Initial calculations predict a large dipole moment for $C_{60}O$, strongly localised close to the oxygen atom, with a partial charge of −0.45 e on the oxygen, and 0.49 e on the nearest carbons, where e is the elementary charge. The four next nearest carbons have partial charges of −0.15 e, and all other carbons remain close to neutral ($-0.03\ \mathrm{e} < q < 0.03\ \mathrm{e}$). This results in a very small Coulomb binding between $C_{60}O$ molecule pairs of 0.006 eV at 3.5 Å (Fig. 2), much lower than the average thermal energy at room temperature (≈0.025 eV). However, pairs of $C_{60}O$ molecules are found to exhibit significant induced dipoles located close to the oxygen atom, leading to a much larger Coulomb interaction between molecules (0.33 eV at 3.5 Å, Fig. 2). The calculated Coulomb binding energy is ≈10 k_BT, compatible with the estimation by Di Biasio et al. [20] for an RLCA mechanism. As these induced dipole interactions diminish rapidly with separation, the energy gradient with distance is much steeper. Induced charges on the righthand side $C_{60}O$ are located on the four nearest carbons to the oxygen atom, favouring spatial arrangements where O approaches $C_{60}O$ cages in an orientation away from another O. Based on these results, we expect the Coulomb binding between a C_{60} and $C_{60}O$ to be similar that of a pair of $C_{60}O$ molecules, shown in Fig. 2. Although solvent interactions are not included in these calculations, which could result in a significantly smaller interaction energy, these results provide an indication of a strong Coulomb binding between $C_{60}O$ molecules. Therefore, from quantum chemical calculations, we can conclude that $C_{60}O$ molecules are expected to bind to other $C_{60}O$ or C_{60} molecules, with the exception of configurations which bring oxygen atoms in close proximity.

Given the low fraction of $C_{60}O_x$ in solution (only ≈0.7% after 21 h light exposure as measured by NMR, Fig. S1, it is unlikely that the clusters comprise solely $C_{60}O_x$, and must thus include a significant fraction of C_{60} within the clusters. This is compatible with our findings from quantum chemical calculations, which indicates binding can take place between $C_{60}O$ and C_{60} molecules.

The predicted low binding energy was evaluated experimentally via two methods: mechanical agitation (Fig. 3a) and thermal energy (Fig. 3b). In short, 0.3% C_{60} solutions were exposed to light and then vortexed or heated to 65 °C while monitored by DLS. [30]

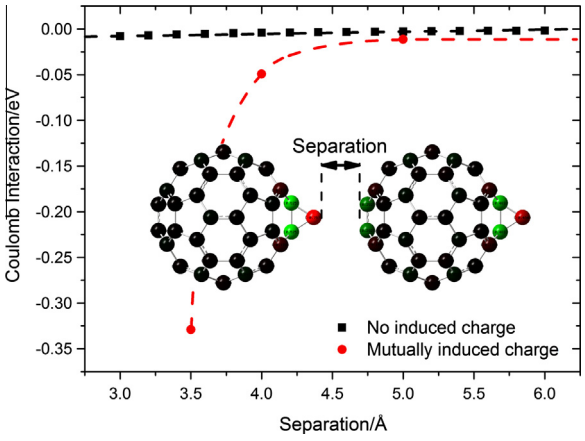

Fig. 2. Calculated energy landscape for separation of $C_{60}O$ molecules in the (■) absence of induced charges, using point charges on a single $C_{60}O$ molecule. Quantum chemical calculation of pairs of $C_{60}O$ molecules taking into account (●) mutually induced charges, expected to occur in this system. Dashed lines are guides to the eye.

Both agitation and thermal stress result in a decrease in amplitude (a_2) back towards the original values for unexposed solutions, indicating cluster dissociation. After the break up of clusters, the oxidised C_{60} solutions were stored at rest, in the dark at 25 °C, and measurements carried out every hour. We find that clusters reform over time, as evidenced by an increase in a_2 over several hours. Such epoxides become solubilised above 50 °C, but precipitate at lower temperatures (additional temperature results are shown in Fig. S4a). The recovery rate of fullerene association appears to correlate with t_{hv}, which is expected since a larger fullerene population, oxidised over longer light exposure times should result in cluster growth at a faster rate.

3.3. Effect of light spectrum and intensity

We next discuss the light exposure requirements for fullerene epoxidation and aggregation to occur. Four different light sources were employed: (i) ambient laboratory light, (ii) high intensity white light, (iii) UV-A lamp and (iv) a HeNe laser (used for the majority of the experiments here), detailed in Section S3. Representative DLS correlation functions obtained with the different sources are shown in Fig. S3, as well as the respective spectral irradiances. We estimate the number of photons based on the power, efficiency and exposure duration of the various light sources and related it to the average value of the DLS correlation function between 4 and 12 μs (and thus to the cluster number density). For a 0.2 wt% C_{60} solution, we estimate that 1 h of ambient laboratory light (measured to be 3.5×0^{13} photons/s/cm^2) exposure is sufficient to form clusters as measured by DLS, shown in Fig. 4a. By contrast, prolonged UV-A exposure (26 h), even with a higher C_{60} concentration (0.3 wt%), did not result in significant cluster formation compared to a sample kept in the dark (the low value for $g^{(2)}(q,t)$ shown in Fig. 4 also includes a small contribution from laboratory light exposure during sample handling). By attenuating the 4 mW HeNe laser power, it can be seen in Fig. 4b that $g^{(2)}$ (and thus the cluster density) increases approximately linearly with increasing light dose (or laser power at constant exposure time). We can thus estimate that only 1 h of ambient laboratory light is sufficient to induce fullerene oxidation and subsequent cluster formation.

3.4. Cluster formation mechanism

To investigate the cluster formation mechanism, a series of additional intermittent laser experiments was carried out, varying the relative light exposure and dark time intervals. The experimental protocol included: (i) continuous light exposure, (ii) 6 min exposure per 26 min, and (iii) 6 min exposure per h, over a period of several days (shown graphically in Fig. S2). In order to interpret the results, we consider the total experimental time, t, and the light exposure time, t_{hv}. Fig. 5a summarises DLS results for the correlation amplitudes a_2 and a_3, as well as cluster hydrodynamic radius $R_{h,2}$. There is a dependence between a_2 and a_3 with light dose (i.e. number of photons), whilst $R_{h,2}$ remains relatively unaffected, for the exposure conditions investigated. This indicates that once the clustering process begins, induced by light exposure and oxidation, clusters ranging in size from 50 to 200 nm appear to grow at the same rate. The values for a_3, corresponding to large micron-sized clusters, indicate that solutions exposed to larger light doses exhibit larger clusters at earlier times. Once ≈100 nm clusters are present, the larger micron-sized clusters grow, whose population depends on light dose. Fig. 5b shows two key aspects of fullerene clustering: while light exposure induces cluster formation, subsequent cluster growth ensues spontaneously in the absence of light corroborating the results shown in Fig. 5a. Fullerene epoxide formation is thus a necessary condition for cluster formation (below

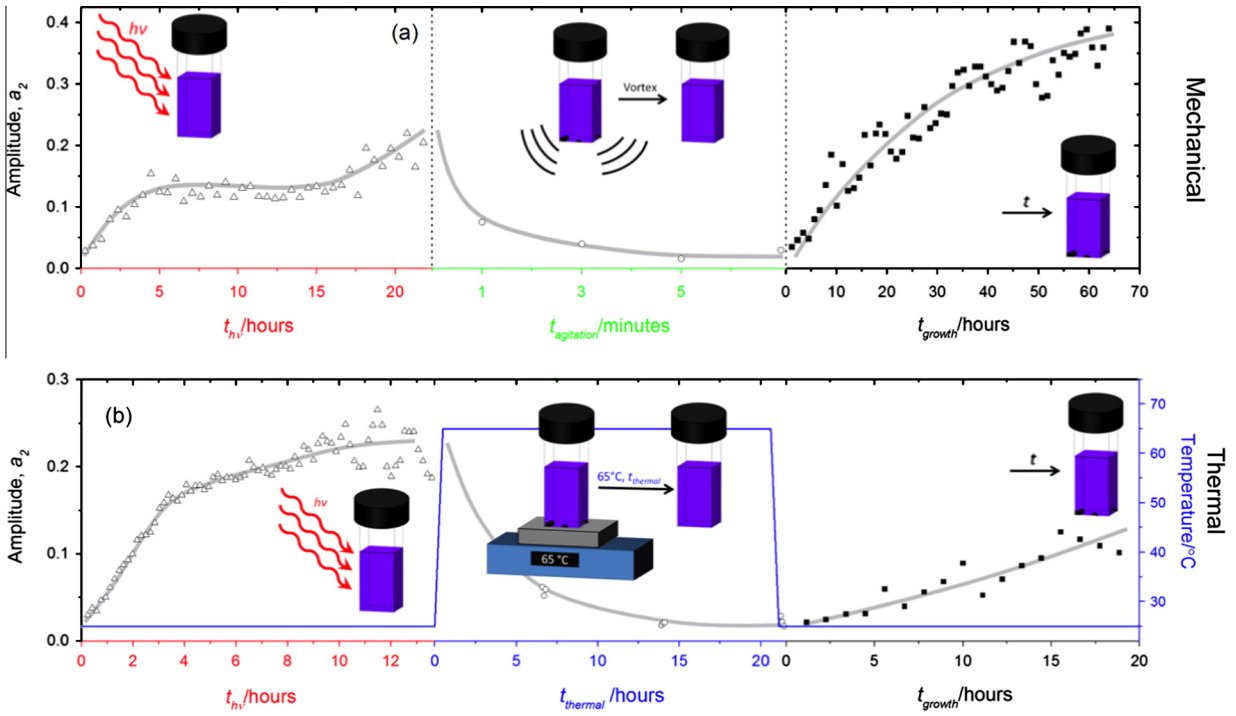

Fig. 3. (a) DLS correlation amplitude, a_2, corresponding to fullerene clusters, obtained using Eq. (1), upon light exposure, mechanical agitation (vortex), and cluster reformation in dark conditions. (b) DLS correlation amplitude a_2 (data points) and corresponding solution temperature (blue line, scale on right axis). Following illumination and cluster formation, the solution was heated in the dark to 65 °C and cooled before measurements resumed. Solutions were stored in the dark and measured every hour (minimising additional oxidation). Our results demonstrate the reversibility of oxidised C_{60} clustering: redissolution by mechanical agitation or increased temperature, and subsequent reformation in their absence. Grey lines are guides to the eye. (For interpretation of the references to colour in this figure legend, the reader is referred to the web version of this article.)

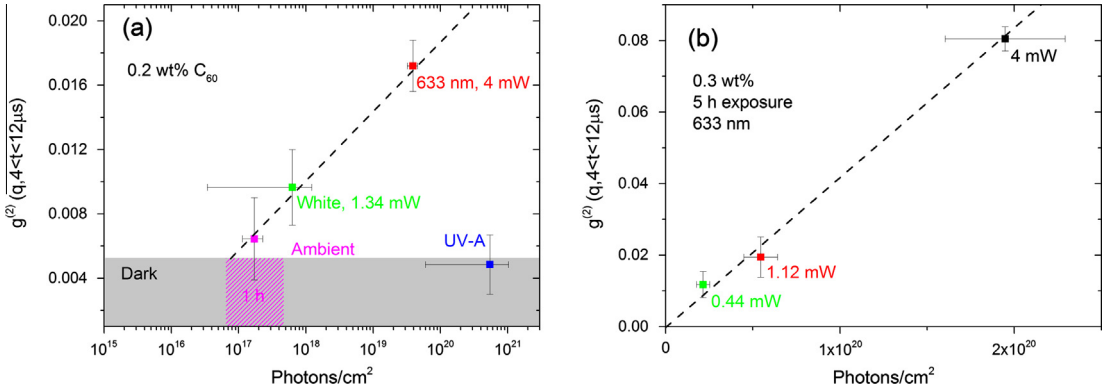

Fig. 4. Dependence of DLS $g^{(2)}(q,t)$ at $4 < t < 12$ μs on number of photons impinging on solution for the various light sources investigated in Fig. S3 (a) 1 h light exposure of 0.2 wt% C_{60}/toluene from 633 nm, 4 mW laser, high intensity white and ambient light, and as before a 0.3 wt% C_{60}/toluene solution was exposed to 365 nm, 100 W UV light for 26 h. (b) 0.3 wt% C_{60}/toluene from 633 nm light at powers ranging from 0.44 to 4 mW.

the C_{60} miscibility limit in toluene), and the growth of C_{60} clusters is slow, taking place even after 10 s of hours in the *absence* of light exposure.

The mechanism for light-induced fullerene cluster formation appears thus to involve an initial photochemical reaction, followed by a slow directional association, resulting in at least two cluster population distributions. Clustering is observed at concentrations down to at least 0.1 wt% (lowest studied) with the kinetics depending strongly on fullerene loading. We rationalise the experimental results as follows. *Stage I*: $C_{60}O_x$ production, characterised in Figs. 1a and b and S1. The yield of this photochemical reaction in dilute solution is inevitably low, as we estimated about 0.7% conversion by NMR after 21 h. *Stage II*: once enough $C_{60}O_x$ is formed, induced dipole interactions between $C_{60}O_x$ and C_{60} result in cluster formation with size ranges of 50–100 nm. Cluster formation appears to have an induction time (≈1 h in the conditions investigated) for a well defined correlation decay to appear in DLS (Fig. 5b, ■). Thereafter, these clusters, likely to contain both $C_{60}O_x$ and C_{60}, and continue to grow in number and size, characterised by a typical $R_{h,2}$ of 100 nm. *Stage III*: Micron-sized large cluster growth. Once a significant number of 100s nm clusters are produced, a decrease in a_2 is observed, accompanied by an increase in a_3 (seen most clearly for $t_{hν} = 15$ h in Tol-O, Fig. 5c). A bi-modal cluster distribution is found at sufficiently long times, with ≃100 nm coexisting with micron-sized clusters, instead of a gradual cluster growth into larger agglomerates. The formation of micron sized clusters is thus likely due to cluster–cluster aggregation, although small intermediate populations cannot be ruled out due to the finite time

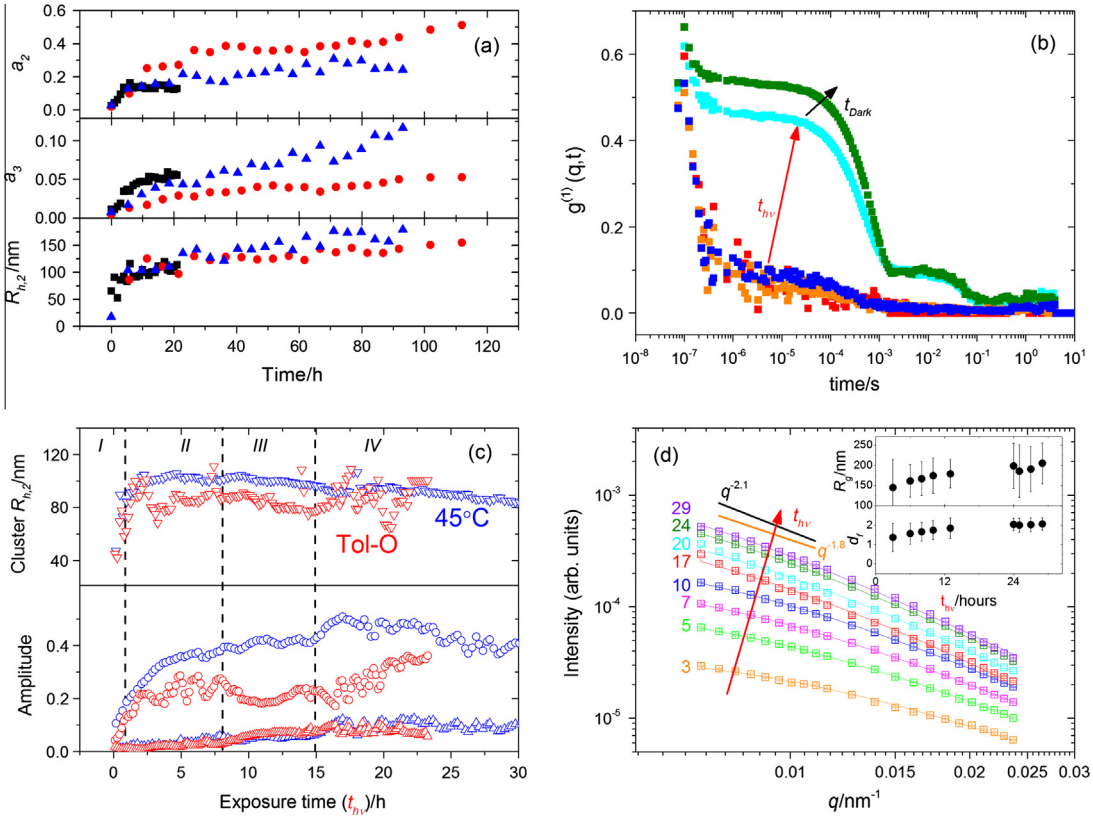

Fig. 5. (a–c) DLS and (d) SLS results of 0.3 wt% C_{60}/toluene solution exposed to a 4 mW, 633 nm laser. (a) (■) continuous light exposure, (△) 6 min exposure per 26 min, and (●) 6 min exposure per h. R_h,2, characterising cluster size, exhibits similar time dependence for all cases, while a_2 and a_3, corresponding to cluster populations, differ. (b) Correlation functions of freshly prepared (■) C_{60} exposed to light for 45 min (■), 1 h (■) and 31 h (■) after which the solution is left in the dark for 12 h (■). (c) DLS results of $R_{h,2}$ ▽, a_2 ○ and a_3 Δ. Comparing different solution conditions, oxygenated toluene (Tol-O) (red) and toluene at 45 °C (blue). (d) SLS data indicating an increasing R_g via a combination of Guinier and fractal analysis [31]; fractal power d_f also increases. Selected data shown in inset. (For interpretation of the references to colour in this figure legend, the reader is referred to the web version of this article.)

resolution and sensitivity of DLS. *Stage IV*: Densification of clusters and precipitation. Fig. 5d shows SLS measurements during cluster formation from which further structural information can be extracted. An average of results from power law, Guinier (in the range $7.1 \leqslant q \leqslant 1.05 \times 10^{-3}$ nm^{-1}) and fractal analysis [31] yield a (fractal) power law d_f and cluster radius of gyration R_g. (The models are discussed in Section S1.4.) A qualitative trend is observed: R_g and d_f increase during cluster formation (inset of Fig. 5d). The R_g follows the same trend as seen for $R_{h,2}$ with R_g increasing from 140 to 200 nm (due to the limited q range (q_{max}/q_{min} <10) and q-range not fully covering $R_g^{-1} < q < R_0$, where R_0 is the radius of individual particles, only estimates for d_f can be obtained).

The increase in d_f is compatible with an aggregation process via monomer–cluster aggregation, which produces denser clusters than cluster–cluster aggregation. A mechanism similar to the 'poisoned' Eden model [23,24], appears likely, as the initial stages of

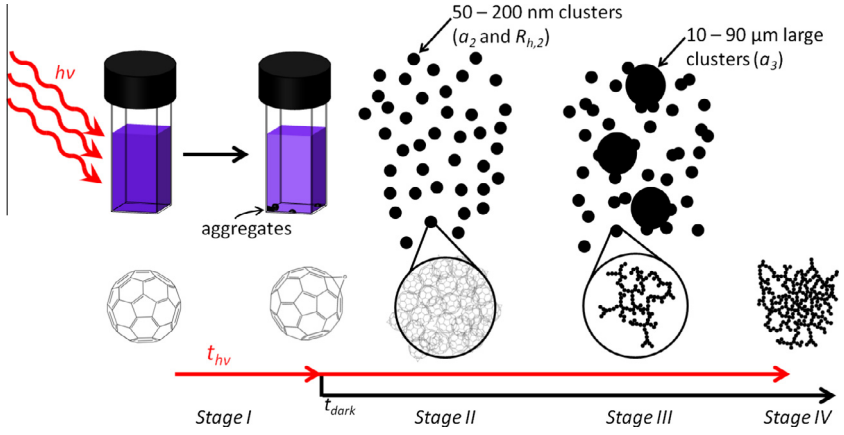

Fig. 6. Schematic depicting light exposure of C_{60}/toluene solutions in ambient conditions, and subsequent formation of fullerene epoxides (*Stage I*), forming clusters of 50–200 nm (*Stage II*) which then grow over time to produce microscopic fullerene particles (*Stage III*) and which further densify over time (*Stage IV*) to form more compact objects.

aggregation are expected to be limited by the formation induced dipoles and restricted by the relative location of oxygen sites. d_f values previously reported for C_{60}/solvent systems include 2.1 for C_{60}/benzene [11] and 1.8–2.4 for C_{60}/water [15]; in our results, d_f increases from 1.34 to 2.05, indicating that clusters become increasingly compact with time, possibly due to C_60 or $C_{60}O_x$ diffusion within 100s nm clusters resulting in further densification and thus higher fractal dimension. Alternatively bond breaking and cluster rearrangement can also result in densification, as suggested in certain cases of protein aggregation [32]. A schematic summarising the proposed light induced cluster formation is given in Fig. 6.

4. Conclusions

We have investigated the light-induced fullerene oxidation and clustering in solution, below the miscibility limit of neat fullerenes. Modest illumination in ambient conditions (c.f. Figs. 4 and S3) was found to cause the formation of fullerene epoxides, confirmed by MS, NMR and FTIR spectroscopies. In order to ensure reproducibility of solution processed fullerene composites and films, light exposure – even to ambient light – must therefore be controlled and reported. Upon oxidation, fullerene solubility decreases resulting in cluster formation with $R_{h,2}$ on the order of 100 nm due to Coulomb interactions. Cluster $R_{h,2}$ can be controlled via concentration, time, solvent, laser power and temperature (Fig. S4). Cluster formation is compatible with a 'poisoned' Eden model and a bimodal cluster population develops and densifies over time. The potential impact of fullerene epoxides lies in organic electronics and industries where fullerenes and their derivatives are commonly processed in solution prior to film formation [33,34]. Light exposure of polymer–fullerene composite films has been shown to profoundly impact their stability and morphology [35–37]. Additionally, fullerene epoxides can be used to synthesise further functionalised fullerenes [38], and this method appears to be relatively simple and scalable for fullerene epoxide production, and could be conducted in a flow reactor [39]. Cluster formation is expected to have significant implications for film formation, fullerene crystallisation and thus for thin film morphology.

Acknowledgments

RD and SF thank the Engineering and Physical Sciences Research Council (EPSRC) for funding (EP/G037515/1). We thank Matthew Allinson for anhydrous toluene and fullerene solution preparation in inert atmosphere, Peter Haycock for ^{13}C NMR spectroscopy, and Him Cheng Wong for spectral measurements of various light sources.

Appendix A. Supplementary material

Supplementary data associated with this article can be found, in the online version, at http://dx.doi.org/10.1016/j.jcis.2015.01.005.

References

[1] W. Krätschmer, L.D. Lamb, K. Fostiropoulos, D.R. Huffman, Nature 347 (6291) (1990) 354–358, http://dx.doi.org/10.1038/347354a0.
[2] A. Rao, P. Zhou, K.-A. Wang, G.T. Hager, J.M. Holden, Y. Wang, X.-X. Bi, P.C. Eklund, D.S. Cornett, M.A. Duncan, I.J. Amster, W.T. Lee, J. Amster, Science 259 (5097) (1993) 955–957. <http://www.jstor.org/stable/2880616>.
[3] P. Zhou, Z.-H. Dong, A.M. Rao, P.C. Eklund, Chem. Phys. Lett. 211 (4–5) (1993) 337–340, http://dx.doi.org/10.1016/0009-2614(93)87069-f.
[4] P. Eklund, A. Rao, P. Zhou, Y. Wang, J. Holden, Thin Solid Films 257 (2) (1995) 185–203, http://dx.doi.org/10.1016/0040-6090(94)05704-4.
[5] J. Wang, J. Enevold, L. Edman, Adv. Funct. Mater. 23 (25) (2013) 3220–3225, http://dx.doi.org/10.1002/adfm.201203386. <http://doi.wiley.com/10.1002/adfm.201203386>.
[6] G. Yu, J. Gao, J.C. Hummelen, F. Wudl, A.J. Heeger, Science 270 (5243) (1995) 1789–1791. <http://www.jstor.org/stable/2888156>.
[7] C. Lanzellotto, G. Favero, M.L. Antonelli, C. Tortolini, S. Cannistraro, E. Coppari, F. Mazzei, Biosensors Bioelectron. 55 (2014) 430–437, http://dx.doi.org/10.1016/j.bios.2013.12.028. <http://www.sciencedirect.com/science/article/pii/S0956566313008993>.
[8] R. Taylor, J.P. Parsons, A.G. Avent, S.P. Rannard, T.J. Dennis, J.P. Hare, H.W. Kroto, D.R.M. Walton, Nature 351 (6324) (1991) 277, http://dx.doi.org/10.1038/351277a0.
[9] L. Juha, J. Krása, L. Láska, V. Hamplová, L. Soukup, P. Engst, P. Kubát, Appl. Phys. B Photophys. Laser Chem. 57 (1) (1993) 83–84, http://dx.doi.org/10.1007/BF00324103. <http://link.springer.com/10.1007/BF00324103>.
[10] F. Cataldo, Polym. Int. 48 (2) (1999) 143–149.
[11] Q. Ying, J. Marecek, B. Chu, Chem. Phys. Lett. 219 (3–4) (1994) 214–218, http://dx.doi.org/10.1016/0009-2614(94)87047-0. <http://www.sciencedirect.com/science/article/pii/0009261494870470>.
[12] Q. Ying, J. Marecek, B. Chu, J. Chem. Phys. 101 (4) (1994) 2665, http://dx.doi.org/10.1063/1.467646. <http://link.aip.org/link/?JCPSA6/101/2665/1>.
[13] Y.-P. Sun, C.E. Bunker, Nature 365 (6445) (1993) 398, http://dx.doi.org/10.1038/365398a0.
[14] Y.-P. Sun, B. Ma, C.E. Bunker, B. Liu, J. Am. Chem. Soc. 117 (51) (1995) 12705–12711, http://dx.doi.org/10.1021/ja00156a007.
[15] Z. Meng, S.M. Hashmi, M. Elimelech, J. Colloid Interface Sci. 392 (2013) 27–33, http://dx.doi.org/10.1016/j.jcis.2012.09.088. <http://www.ncbi.nlm.nih.gov/pubmed/23211871>.
[16] R. Koeppe, N.S. Sariciftci, Photochem. Photobiol. Sci. 5 (12) (2006) 1122–1131, http://dx.doi.org/10.1039/b612933c. <http://pubs.rsc.org/en/Content/ArticleHTML/2006/PP/B612933C>.
[17] R.S. Ruoff, D.S. Tse, R. Malhotra, D.C. Lorents, J. Phys. Chem. 97 (1993) 3379–3383.
[18] J. Jeong, W.-S. Kim, S.-I. Park, T.-S. Yoon, B.H. Chung, J. Phys. Chem. C 114 (30) (2010) 12976–12981, http://dx.doi.org/10.1021/jp103875s.
[19] P. Meakin, in: H.E. Stanley, N. Ostrowsky (Eds.), On Growth and Form, Martinus Nijhoff Publishers, Dordrecht, 1986, pp. 11–135. Ch. 5.
[20] A. Di Biasio, G. Bolle, C. Cametti, P. Codastefano, F. Sciortino, P. Tartaglia, Phys. Rev. E 50 (2) (1994) 1649–1652, http://dx.doi.org/10.1103/PhysRevE.50.1649.
[21] M. Eden, in: 4th Berkeley Symposium on Mathematical Statistics and Probability, 1961, pp. 223–239.
[22] T. Witten, L. Sander, Phys. Rev. Lett. 47 (19) (1981) 1400–1403, http://dx.doi.org/10.1103/PhysRevLett.47.1400.
[23] K. Keefer, D. Schaefer, Phys. Rev. Lett. 56 (22) (1986) 2376–2379, http://dx.doi.org/10.1103/PhysRevLett.56.2376.
[24] K.D. Keefer, MRS Proc. 73 (1986) 295–304, http://dx.doi.org/10.1557/PROC-73-295. <http://journals.cambridge.org/abstract_S1946427400553238>.
[25] D. Asnaghi, M. Carpineti, M. Giglio, MRS Bull. (1994) 14–18.
[26] D.I. Schuster, P.S. Baran, R.K. Hatch, A.U. Khan, S.R. Wilson, Chem. Commun. (22) (1998) 2493–2494, http://dxdoi.org/10.1039/a806603e. <http://pubs.rsc.org/en/content/articlehtml/1998/cc/a806603e>.
[27] K.M. Creegan, J.L. Robbins, W.K. Robbins, J.M. Millar, R.D. Sherwood, P.J. Tindall, D.M. Cox, J.P. McCauley, D.R. Jones, J. Am. Chem. Soc. 114 (3) (1992) 1103–1105, http://dx.doi.org/10.1021/ja00029a058.
[28] R. Nizam, S.M.A. Rizvi, A. Azam, J. Nanotechnol. Eng. Med. 2 (1) (2011) 011015, http://dx.doi.org/10.1115/1.4003305.
[29] Y. Tajima, K. Takeuchi, C60O3 Fullerene Triepoxides with C1, C2, or Cs Symmetry; Separation by Two-Step Column Chromatography First with Silica Gel and Then With a Substance Having p–p Interactions Such As Pyrene-Modified Silica Gel, 2005. <http://www.google.com/patents/US20050154219>.
[30] Specifically, one solution was light exposed for 21 h, and then mechanically agitated using a vortexer at 3000 rpm for 7 min. A separate solution was light exposed for 13 h and heated to 65 °C for nearly 21.5 h while monitored by DLS.
[31] J. Teixeira, J. Appl. Cryst. 21 (6) (1988) 781–785, http://dx.doi.org/10.1107/S0021889888000263. <http://scripts.iucr.org/cgi-bin/paper?S0021889888000263>.
[32] V.J. Anderson, H.N.W. Lekkerkerker, Nature 416 (6883) (2002) 811–815, http://dx.doi.org/10.1038/416811a.
[33] B.C. Thompson, J.M.J. Fréchet, Angew. Chem. (International ed. in English) 47 (1) (2008) 58–77, http://dx.doi.org/10.1002/anie.200702506. <http://www.ncbi.nlm.nih.gov/pubmed/18041798>.
[34] A. Montellano López, A. Mateo-Alonso, M. Prato, J. Mater. Chem. 21 (5) (2011) 1305, http://dx.doi.org/10.1039/c0jm02386h. <http://pubs.rsc.org/en/content/articlehtml/2011/jm/c0jm02386h>.
[35] H.C. Wong, A.M. Higgins, A.R. Wildes, J.F. Douglas, J.T. Cabral, Adv. Mater. 25 (7) (2013) 985–991, http://dx.doi.org/10.1002/adma.201203541.
[36] Z. Li, H.C. Wong, Z. Huang, H. Zhong, C.H. Tan, W.C. Tsoi, J.S. Kim, J.R. Durrant, J.T. Cabral, Nat. Commun. 4 (2013) 2227, http://dx.doi.org/10.1038/ncomms3227.
[37] H.C. Wong, Z. Li, C.H. Tan, H. Zhong, Z. Huang, H. Bronstein, I. McCulloch, J.T. Cabral, J.R. Durrant, ACS Nano http://dx.doi.org/10.1021/nn404687s. <http://pubs.acs.org/doi/abs/10.1021/nn404687s>.
[38] Y. Tajima, K. Takeshi, Y. Shigemitsu, Y. Numata, Molecules 17 (6) (2012) 6395–6414, http://dx.doi.org/10.3390/molecules17066395. <http://www.mdpi.com/1420-3049/17/6/6395>.
[39] J.H. Bannock, S.H. Krishnadasan, M. Heeney, J.C. de Mello, Mater. Horizons 1 (4) (2014) 373, http://dx.doi.org/10.1039/c4mh00054d. <http://pubs.rsc.org/en/content/articlehtml/2014/mh/c4mh00054d>.